Chapter 8: Simulating the thermal impact of building-integrated agriculture on the built environment[5]

1. Introduction

This chapter concludes the third research objective as the final aspect to assess the climate change adaptation (CCA) potential of building-integrated agriculture (BIA) as a building retrofitting strategy. The final objective set out to simulate the potential of BIA to improve the heating and/or cooling loads of the built environment if subjected to hotter climate change-driven conditions. This chapter builds on the findings discussed in Chapter 7, during which an experiment collected data on the thermal performance of five rooftop greenhouses (RTGs) located in Tshwane and Johannesburg. The data collected during the experiment enabled the validation of a digital simulation, allowing for further simulations that would otherwise have been impossible to document in reality (Groat & Wang 2013).

A number of studies have considered response strategies to the expected impacts of climate change, such as the work conducted by Smith (2010) that identifies the required changes to building practices in the UK and discusses in detail adjustments to walls, roofs, window and door constructions. A comprehensive study undertaken by Gething and Puckett (2013) also considers adjustments needed to UK buildings in response to expected climate change impacts; this includes documenting and assessing their future performance through modelling methods. The potential to retrofit the existing built environment to improve their performance has also been considered in many studies. Carnielo and Zinzi (2013) and Santamouris (2013) propose changing the albedo factor of sidewalks to curb the impact of UHI in urban contexts. Carnielo and Zinzi (2013) conclude that the strategy has beneficial impacts by quantifying lower temperatures and its resultant cooling impact on the city. A study by Kleerekoper et al. (2015) also tests using facade colours to increase local updrafts as a cooling measure in the urban context. In the South African context, Conradie (2017) modelled the cooling impact of external shading on buildings, providing guidance on how these can be retrofitted to adjust the built environment to climate change impacts.

In terms of the urban agriculture (UA) discourse few studies appraise the impact of retrofitting the built environment with BIA projects. Specht et al. (2014) conducted a systematic literature review to identify the social, economic and ecological benefits and limitations of BIA. Goldstein et al. (2016) build on the previous reviews of BIA and identify a series of ecological benefits in

[5] An article was developed from this chapter and is currently under review:
Hugo, JM, du Plessis, C & Masenge, A. Retrofitting Southern African cities: a call for appropriate rooftop greenhouse designs as climate adaptation strategy.

cases where UA is closely integrated with the built environment. Several recent studies have conducted LCA's to quantify the environmental impact of RTGs that are specifically integrated with the built environment (Benis et al. 2017; Nadal et al. 2017; Sanye-Mengual et al. 2018).

This chapter continues to assess the performance of retrofitting BIA farms to the built environment as CCA strategies. The specific focus is to quantify the thermal impact of RTGs on the built environment in the South African interior. The chapter starts by discussing the model parameters for the multiple models used in the study. It continues to discuss the results obtained from the simulations and finally postulates the drivers of the resultant impacts.

2. Description of the simulation models

The research method to experiment and collect data in order to validate a simulation has been undertaken by a number of studies (e.g. Taleghani, et al. 2014; Kleerekoper et al. 2017); a specific method followed by Skelhorn et al. (2016) informed the research protocol. Skelhorn et al. (2016) considered the impact of the urban morphology on the microclimate. This was used to develop alternative place-specific weather files. This was subsequently used to model the building's performance within adjusted climate conditions.

This simulation process consisted of a two-phased process. The first phase involved the modelling of an RTG that was documented during the fieldwork (refer to Chapter 7). In this case, the Stanop Building (SB) farm was used as the test-case that is least affected by the surrounding built environment. Using the real-world example allowed for the validation of the RTG modelling parameters. Once validated, the study commenced with the second simulation phase that considered the impact of a RTG on a typical office building in Hatfield, Tshwane. Details regarding the research method are discussed in Chapter 3.

2.1. Simulation phase 1

2.1.1. Model description – Model of the microclimate to develop the weather file of the microclimate.

Using EnviMet as modelling programme the basic spatial and material conditions of the SB farm site were documented (Figure 92). This included modelling the building and the surrounding city blocks (Figure 93). In Tables 48 and 49 the material characteristics are discussed; these were observed on site and defined in the software to replicate the existing conditions. At the time of the study the EnviMet methodology was deemed a highly accurate method to model microclimatic changes affected by the local meteorological factors, vegetation, and the built structures and material-use of the urban environment (Kleerekoper et al. 2017; Skelhorn et al. 2016).

Figure 92: Stanop Building and its context (Source: Googlemaps).

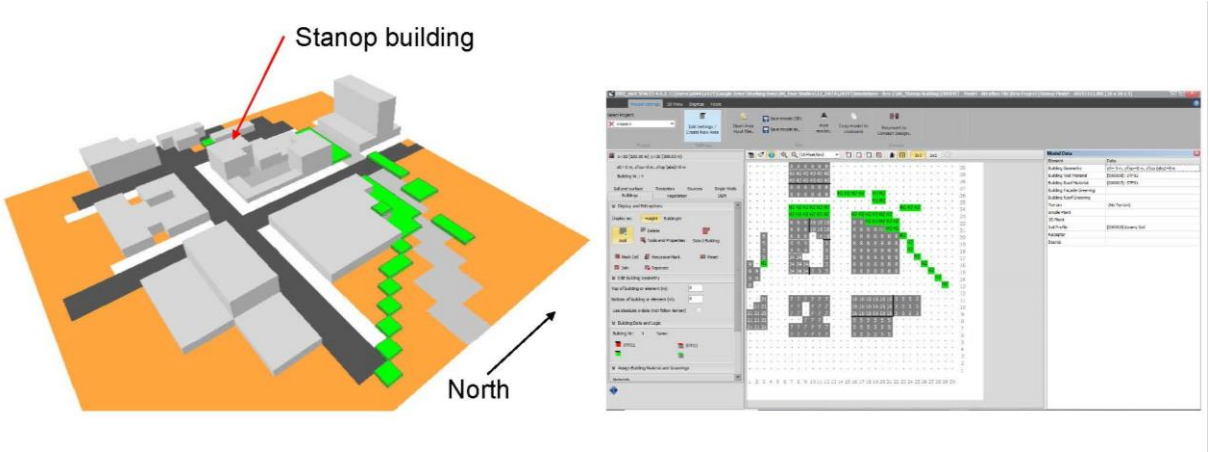

Figure 93: Envimet Model of the Stanop Building and surrounding context.

The Envimet models were modelled on a 10x10 metre grid. Using the larger grid proved feasible within the computational constraints and had limited impact on the outcomes needed from the analysis. During the initial simulations the Johannesburg (JHB) climate file was used as full forcing file to set the meteorological parameters, but the simulation output did not account for the large diurnal thermal swing documented on site. In response, it was decided to employ a simple forcing file using the maximum and minimum temperatures measured on site as parameters. The resultant microclimate conditions were correlated with the measured data from the site.

Before commencing with the correlation analysis the data were tested for normality using a histogram and descriptive statics in Microsoft Excel. Due to software limitations a Shapiro-Wilk test was not conducted to test for normality. For both data sets the mean and median did not differentiate with more than 0.4°C. The skewness for both data sets was less than 1, which is acceptable for normal distribution as suggested by Abbott (2017). The kurtosis for the measured data set was normal, while the modelled data set was slightly leptokurtic. Based on the normality test findings, it was assumed with a high degree of certainty that the data has a normal distribution.

The correlation between the model and measured temperatures was tested using Pearson's R method. A final correlation coefficient of 0.79 was achieved. Upon validating the Envimet model, the microclimatic differences between the ground and roof levels were determined. This informed the adjustments made to the JHB weather file (available from EnergyPlus) to develop an appropriate microclimate weather file. This adjusted weather file was used in the subsequent IESve model to validate the RTG model parameters.

Table 48: Description of material characteristics used in the SB farm model.

Site	Stanop Building			
Location:	57 Sivewright Avenue in New Doornfontein, JHB			
Coordinates:	26°11'54,16"S			
	28°03'24,02"E			
Building	7 floors			
Components:	**Description**	**Material**	**Colour & (Absorptivity [α])**	**Thickness (m)**
Concrete Surface	Floor of farm	Concrete	Silver (0.2)	0.255 (assumed)
Masonry Wall	High surrounding walls	Plastered and painted masonry	Brown (0.5); White (0.25); Beige (0.3); Grey (0.5)	0.26
Infill	Infill walls	Face-brick masonry	Brown (0.5)	0.24
Steel Roof	Grey painted Steel	Painted Steel	Grey (0.5); Blue (0.7); Galvanised (0.25); Brown (0,5)	0.001

Table 49: Description of material characteristics used in the SB farm model (continued).

Concrete Surface	**Transmission**	**Emissivity**	**Specific Heat Modules J/kg*K**	**References**
Concrete Surface	0	0.85	880	Berge (2009); Engineering Toolbox (2019); ASHRAE (2017)
Masonry Wall	0	0.93	840	
Infill	0	0.93	840	
Steel Roof	0	0.93	940	

2.1.2. Model description – Validation of the RTG characteristics

This simulation step formed part of the initial phase (Phase 1) during which the model parameters of the typical RTG was developed and validated. It used the adjusted weather file developed from the microclimate modelling and modelled the specific conditions documented at the Stanop Building site (Figure 94).

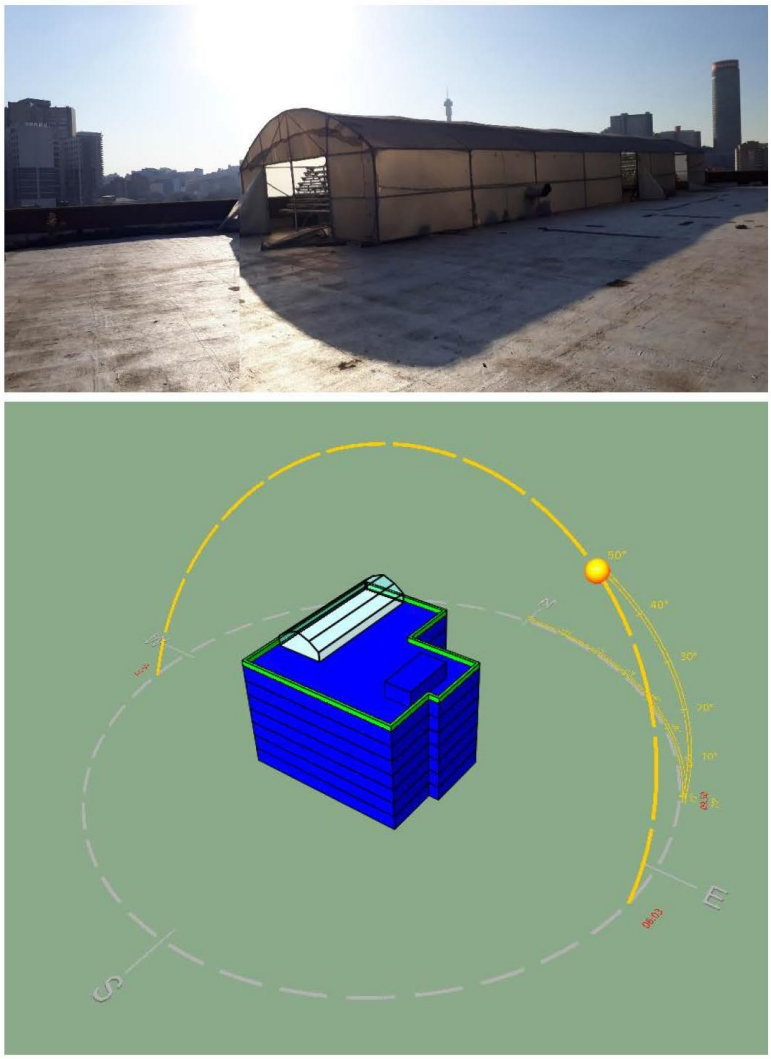

Figure 94: Stanop Building Farm and a three-dimensional view of the IESve model.

The simulation modelled a typical RTG based on the observations made on site (Tables 50, 51 & 52). The RTG did not use any active climate control measures, nor were specific passive strategies incorporated in the design. It was noted that air exchange predominantly takes place through high air infiltration rates due to the poorly sealing envelope. The RTG is also not integrated with the building to facilitate any energy or resource exchanges. As for the material use, the RTG structure was covered in a combination of HDPE shade netting layered on top of a PolyEVA lining.

The construction materials identified on site were confirmed by the contractor that built the greenhouses. The greenhouse membrane consisted of 40% Agri-shade netting (Knitted HDPE monofilament netting) layered on top of 200 micron plastic (White Polyethylene Vinyl Acetate) (see table 52) (Sheppard, 2019). The membrane was tied to a vaulted galvanised steel structure, made from circular hollow steel sections, that was constructed off-site, assembled on-site, and bolt fixed to the concrete roof substrate.

The material characteristics of the Agri shade netting were derived from a number of studies. The basic conductivity coefficient, density and material thickness were derived from Berge (2009), the Engineering Toolbox (2019), and product supplier (SA shadecloth 2019). The absorptivity coefficient (α) was derived from the product suppliers' information (Sheppard, 2019). Work by Abdel-ghany (2011) and Abdel-ghany et al (2014) measured the reflectivity and associated emissivity of shade netting and confirmed the reflectivity as 0.08.

The material characteristics of the white Poly-EVA are more complex. Similar to shade netting, the conductivity coefficient, density, and material coefficient were derived from Berge (2009), Engineering Toolbox (2019) and local product suppliers (Eco-tunnels 2019; PP Plastics 2019; Sunrise Agrifarm 2019). While the light transmittance was derived from product suppliers specifications, the initial absorptivity and reflectance of the Poly EVA lining were derived from a study conducted by Nijskens et al. (1984). As Nijskens et al. (1984) used material characteristics developed under laboratory conditions, after a number of simulations it was concluded that the ageing and dust settling on the greenhouse membrane affected the final reflectivity and absorptivity. The final figures of α=0.45 and r=0.55 were derived from photographs and calculating the absorptivity factor using Image J and a reference surface (Conradie 2017).

The infiltration rate was not measured on site, but adjusted and derived from the simulation model. As the only adjustable parameter, the model started with an air-change rate of 10 as per SANS 10400 – O standards (South African building standards that define acceptable minimum ventilation rates in the built environment). During the fieldwork it was observed that the envelope has multiple gaps and openings, therefore a high air-change rate per hour (ACH) for infiltration was assumed. A literature review on infiltration rates noted a global trend prescribing ACH rates of less than 1 (Leivo et al. 2017). However, the average ACH rates vary considerably between countries, ranging from 3-4 ACH in Sweden (Mattson 2006), to between 0.5 to 83 ACH in a study conducted by Sherman and Dickerhoff (1998). Finally, a study by Persily (1999) assessed the air-tightness of buildings in the US and concluded that the range of ACH rates is extensive, documenting instances of up to 35 ACH. During the simulation and verification process, an infiltration rate of 30 ACH was identified as most reflective of the temperature variations documented on site (Table 50).

Table 50: Description of the RTG validation model.

Model	Rooftop Greenhouse Validation model	References
Location	Stanop building, New Doornfontein, Johannesburg	
Building	7 Storeys	
Greenhouse	Area: 216 m^2 Volume: 744 m^3	
Occupation	108m^2 per person	Observed on site
Occupation Schedule	5 Hours daily.	Observed on site
Modelling parameters	No additional cooling No additional Heating No windows or doors (opening on regular intervals) No additional artificial lighting	Observed on site
Planting	Hydroponic NFT system Area: 104 m^2 , coverage 0.48	Observed on site
Transpiration impact	Latent energy – 9.36 Watts/m^2 adjusted to 0.48 coverage (19.6W/m^2 x 0.48) Based on FOA-PM equation. *Schedule adjusted to accommodate daily fluctuations.* *Schedule adjusted to accommodate seasonal impact.*	Monteith (1965); Allen et al. (1998); Graamans et al. (2018)
Energy load	Electrical water pumps 1.3 Watts/m^2	Observed and assumed.
Greenhouse construction	Floor: 255mm concrete slab with waterproofing – U-Value: 2.617 Composite greenhouse membrane: Knitted HDPE monofilament netting layered on White Poly Ethelyne Vinyl Acetate (Additional information on construction in tables 51 & 52)	Nijskens et al. (1984); Berge (2009); Abdel-ghany (2011); ASHRAE (2017); Engineering Toolbox (2019) and observations on site.
Construction	Construction of building materials delimited from model analyses.	
Ventilation	No artificial ventilation No Natural ventilation Infiltration adjusted to validate model – 30ACH	Observed on site.

Table 51: Construction material parameters of the rooftop greenhouses.

Components:	Description	Material	Colour	Thickness
Shade netting	Greenhouse screen - 40% shading	Knitted HDPE monofilament	Black	0.002mm (model min 1mm)
Plastic Lining	200 microns Greenhouse plastic lining	Polyethylene Vinyl Acetate (Poly-EVA)	White	0.0002mm (model min 1mm)

Table 52: Construction material parameters of the rooftop greenhouses (continued).

Components:	Absorption (α)	Transmission	Reflection (r)	Specific Heat Modules J/kg*K	Thermal Conductivity Coefficient (k)	Density - kg/m^3
Shade netting	0.4	0.6	0.08	1250	0.51	940
Plastic Lining	0.45	0.45	0.55	1250	0.33	940

2.2. Simulation phase 2

2.2.1. Model description – Model of the office building

The simulated building is a theoretical building located in Hatfield (Tables 53, 54, 55 & 56). A multi-storey office building was modelled, as one of the predominant building types of the Hatfield neighbourhood. Furthermore, this building type was chosen as this function presents homogeneity in its building construction and layout. Residential and commercial building functions were excluded due to their diversity in occupation patterns and scheduled use, and in Hatfield commercial functions do not typically occupy complete multi-storey buildings.

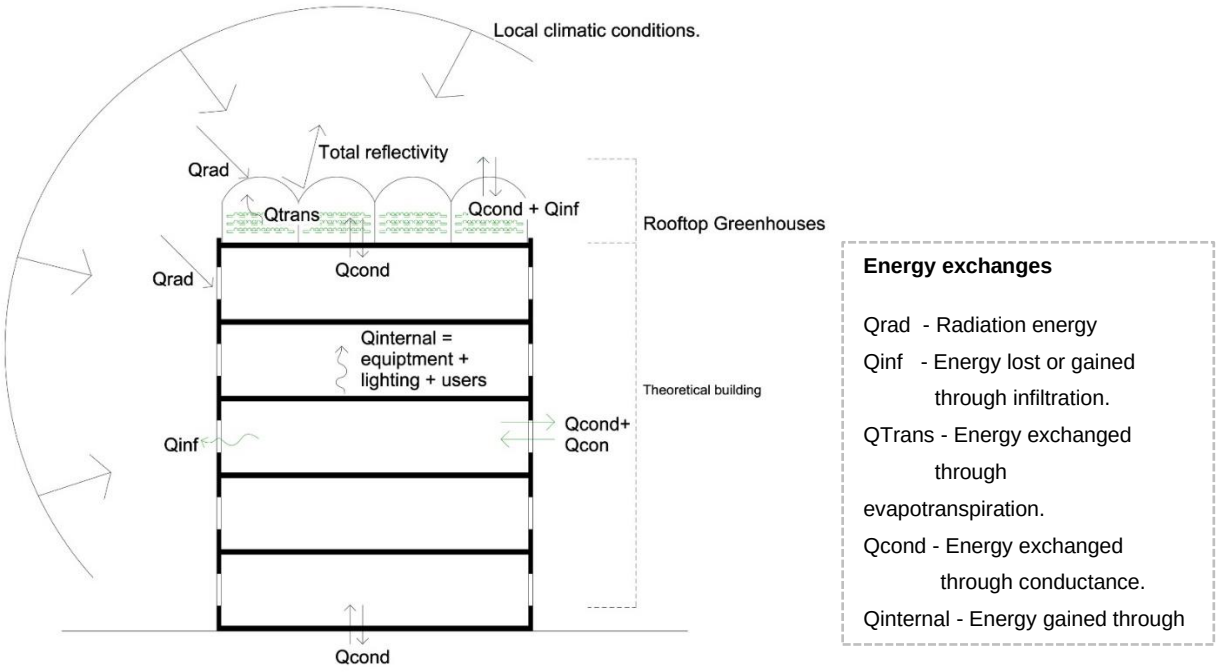

Figure 95: Typical section of thermal envelope of the theoretical building and the energy exchanges considered in the model.

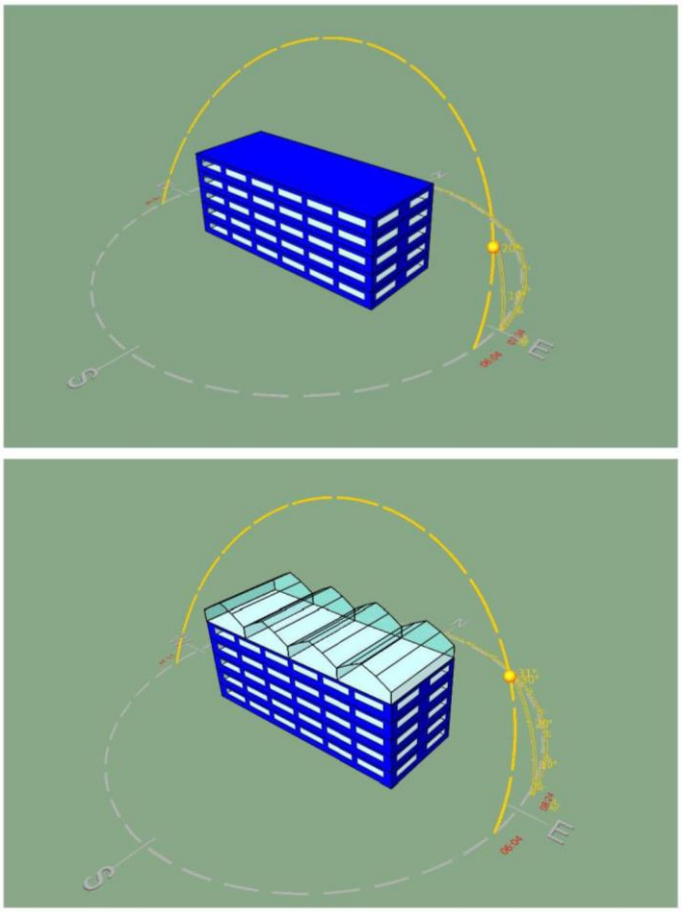

Figure 96: Three-dimensional views of the theoretical retrofitted and non-retrofitted models developed in IESve.

A five-storey building was modelled, based on the average building heights of the neighbourhood (Figures 95 & 96). While the floor plates of the existing buildings are often much larger than 570m^2, the model followed a typical north-facing structure with similar façade configurations on all sides to limit the impact of other design decisions. The weather file used in the modelling was generated for the Hatfield neighbourhood and simulated the current and future adjusted climate change conditions (A2 conditions). The A2 climate change conditions were derived from a number of scenarios developed to forecast expected climate change impacts (IPCC 2000; DEA 2013). In the South African context the A2 scenario is considered a business-as-usual scenario where little climate change mitigation (CCM) is undertaken. As a result average temperature increases of above 4°C are expected with dryer summer rainfall conditions in the western to north-western regions of the country (DEA 2013).

Four types of model variations were developed (Figure 97). This included two primary baseline models with and without RTGs. This allowed one to compare the impact of RTGs on the building performance. Furthermore, two of the models (including and excluding RTGs) represent a typical poorly insulated building constructed prior to the promulgation of SANS 10400XA building standards. The remaining two models are typical SANS10400XA compliant structures (Table 54).

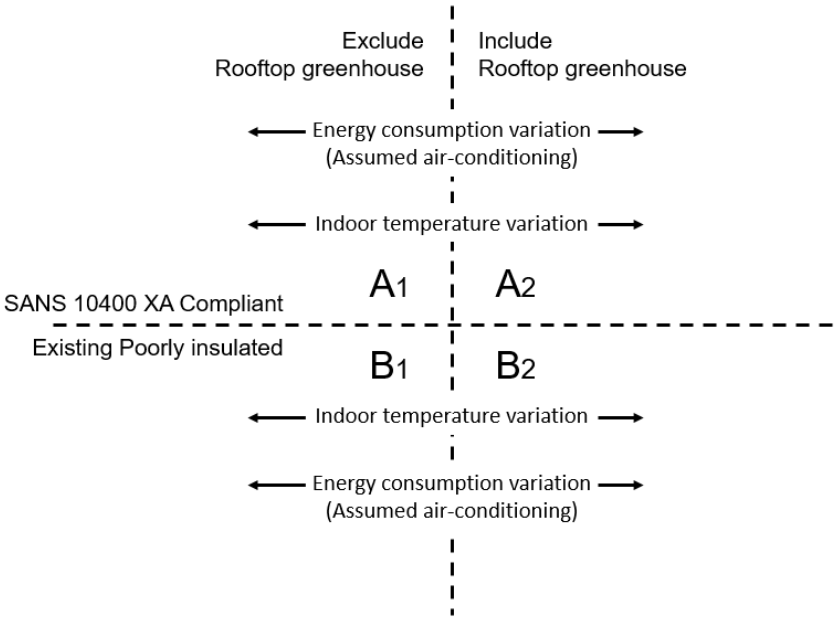

Figure 97: Comparison of the four models in order to model the impact of RTGs on the indoor environment and the subsequent energy use.

To understand the thermal impact of RTGs on a building, a series of simulations was run without any mechanical ventilation or air-conditioning (Table 56). During these simulations the

temperature variations were compared. It is important to note that the models did not intend to achieve thermal comfort, but only tested the impact on the dry-bulb temperature.

In further analyses, the energy consumption impact was tested, by simulating a basic air-conditioning system that controls the indoor environment of the four models (Table 56). The heating and cooling set-points were specified as per SANS 10400-XA standards at 19 and 25°C. Similarly, the air-conditioning system used a typical system as identified in the recent report by the Department of Energy and UNDP entitled *Market assessment of residential and small commercial air-conditioners in South Africa* (DOE, 2019). As a result, the energy variations due to the impact of RTGs were documented and not the optimal air-conditioning design.

Table 53: Model description of the theoretical office building in Hatfield.

Model	Typical Office building (Theoretical Building)	References
Location	Tshwane, Gauteng	
Building	5 Storeys	
Total Floor area	Area: 2 850 m^2 Volume: 8 550 m^3	
Coverage	570 m^2	
Building Occupancy	Office – G1	SANS 10400-A
Occupation	15m^2 per person	SANS 10400-A
Occupation Schedule	8h per day / 5 days per week	SANS 10400-XA
Basic Thermal loads	People –Sensible 70W and Latent 55W Plug load density* – 15W/m^2 Lighting power density* – 12W/m^2 *In the study the lighting and equipment energy was assumed to be converted 100% to sensible thermal gain and 0% to latent thermal gain.	SANS 10400-XA; Harris (2012); ASHRAE (2017)
Model Variations	A1 – Construction is SANS 10400 XA compliant and excludes rooftop greenhouse. A2 – Construction is SANS 10400 XA compliant and includes rooftop greenhouse. B1 – Construction is assumed poorly insulated building and excludes rooftop greenhouse. B2 – Construction is assumed poorly insulated building and includes rooftop greenhouse.	SANS 10400 XA Assumed characteristics.
Ventilation Variations	All models tested under natural ventilation conditions (no additional temperature amelioration tactics included). All models tests under air-conditioning (basic air-condition parameters assumed for comparison)	SANS 10400; Skelhorn et al. (2016); DOE (2019)

Table 54: Description of the construction materials parameters used in the theoretical building in Hatfield.

Models	**A1 & A2 – SANS 10400 XA compliant**	**B1 & B2 – SANS 10400 XA non-compliant**	**References**
Ground Floor	100mm Concrete slab (No insulation) R-value = 0.79; U-value: 1.273	100mm Concrete slab (No insulation) R-value = 0.79; U-value = 1.273	SANS 10400 XA & assumed conditions
First Floor (all other floors)	255mm reinforced concrete slab R-Value = 0.38; U-Value = 2.617	255mm reinforced concrete slab R-Value = 0.38; U-Value = 2.617	Assumed conditions
Walls	230mm masonry wall, plastered on both sides. R-value = 0.48; U-value = 2.607* **SANS 10400 stipulates 230mm masonry wall complies.*	230mm masonry wall, plastered both sides. R-value = 0.48; U-value = 2.607	SANS 10400 XA
Roof	255mm Concrete slab with 120mm expanded polystyrene insulation and waterproofing. R-value = 3.76; U-value = 0.266	255mm Concrete slab with 30mm expanded polystyrene insulation and waterproofing. R-value = 1.19; U-value = 0.841	SANS 10400 XA & assumed conditions
Glazing (30% glazing ratio)	Aluminium frame, double pane (double glazing) (6mm clear glass) - U-value = 2.876; SHGF = 0.78	Aluminium frame, single pane (single glazing) (6mm clear glass) - U-value = 5.17; SHGF = 0.78	SANS 10400 XA & assumed conditions
Greenhouse construction parameters – see table 55 (continued)			

Table 55: Rooftop greenhouse simulation model description.

Model	Rooftop greenhouse on typical office building	References
Greenhouse	Area:570 m^2 Volume: 1963 m^3	
Occupation	108m^2 per person	Table 50
Occupation Schedule	5 Hours daily.	Table 50
Modelling parameters	No additional cooling No additional Heating No windows or doors (opening on regular intervals) No additional artificial lighting	Table 50
Planting	Hydroponic NFT system Area: 274 m^2 , coverage 0.48	Table 50
Transpiration impact	Latent energy – 9.36 Watts/m^2 adjusted to 0.48 coverage (19.6W/m^2 x 0.48) Based on FOA-PM equation. *Schedule adjusted to accommodate daily fluctuations.* *Schedule adjusted to accommodate seasonal impact.*	Monteith (1965); Allen et al. (1998); Graamans et al. (2018)
Energy load	Electrical water pumps 1.3 Watts/m^2	Table 50
Greenhouse construction	Floor: Adjusted as per models A1, A2, B1 & B2 – U-Value: 2.617 Composite greenhouse membrane: Knitted HDPE monofilament netting layered on White Poly Ethelyne Vinyl Acetate (Additional information on construction in tables 32 & 33)	Nijskens et al. (1984); Berge (2009); Abdel-ghany (2011); ASHRAE (2017); Engineering Toolbox (2019) and Table 50
Ventilation	No artificial ventilation No Natural ventilation Infiltration adjusted to validate model – 30ACH	Observed on site.

Table 56: Description of the natural and artificial ventilation parameters of the theoretical building in Hatfield.

Models	**A1 & A2 – SANS 10400 XA compliant**	**B1 & B2 – SANS 10400 XA non-compliant**	**References**
Natural Ventilation	Simple Cross ventilations strategy - 7.5 L/s per person – *no additional strategy followed*		SANS 10400-O
Air infiltration	Highly sealed - 0.25l/s/m^2	Poorly sealed 7.13l/s/m^2	Skelhorn et al. (2016) Persily (1999)
Air-conditioning Heating	SEER – 3.4 SCOP – 3.4 Heating Set point - 19°C		DOE (2019) (Dirker, 2020) SANS 10400-XA
Air-conditioning Cooling	EER – 2.5 SEER – 2.125 Cooling Set point - 25°C		(DOE 2019) (Dirker, 2020) SANS 10400-XA

3. Simulation findings

3.1. Thermal variation models A1 and A2

The analysis compared the thermal variations of the top floors between models A1 (SANS 10400XA compliant without RTGs) and A2 (SANS 10400XA compliant with RTGs). The indoor dry-bulb temperatures, along with the outdoor ambient temperatures were compared for a number of weeks during a typical year. These included a week in the hottest and coldest months of the year, as well as a week during the summer and winter solstices, and equinox periods. The assessment concluded that while there is a limited degree of thermal variation between the models, the retrofitting strategy often leads to a cooler indoor environment.

The visual assessment of the various weeks revealed a slightly cooler indoor environment resulting from the RTGs retrofitted to the existing structure (Model A2) (Figure 98). While the September and December periods have highly correlated thermal conditions; the March and June periods reveal a cooler indoor environment. A correlation analysis between the temperature variations (indoor temperatures of models A1 and A2) conveyed a close correlation between the two models ranging from 0.92 to 0.95 (Pearson's R) (see table 57). During the hottest period in January the correlation coefficient is 0.84. This revealed a small difference in indoor temperatures due to the retrofitted RTGs (model A2) with the largest difference in January being the hottest period.

Table 57: Correlational analysis of the specific weeks simulated in models A1 and A2.

Period of measurement	Pearson's R	Coefficient of Correlation
December 20-27	0.92	89%
January 20-27	0.84	71%
March 20-27	0.92	85%
June 20-27	0.93	86%
July 20-27	0.95	91%
September 20-27	0.94	89%

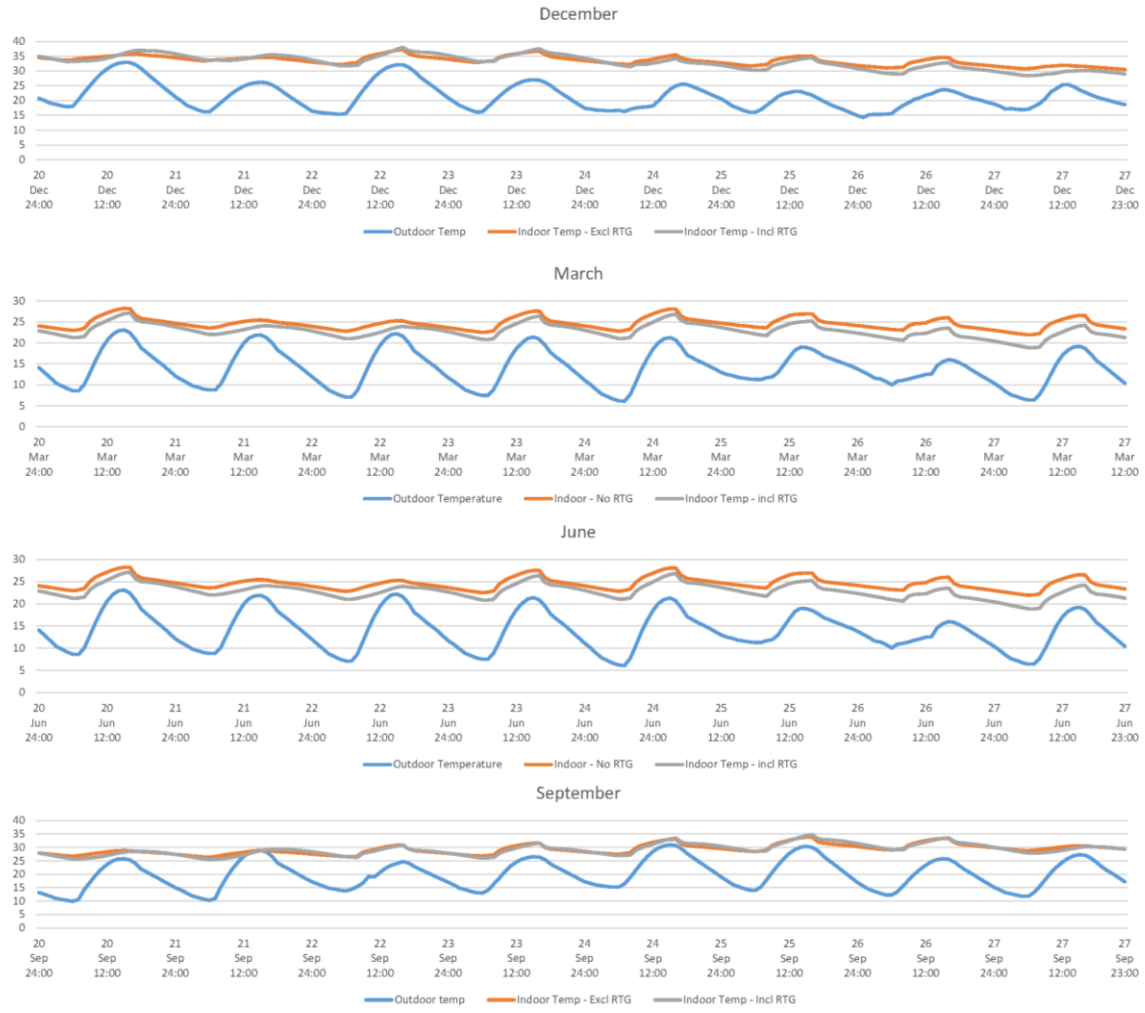

Figure 98: Comparison of the thermal variations between models A1 and A2.

The average ambient temperatures of the top floor, during the prescribed weeks, were calculated for the two models (A1 and A2). The analysis revealed a generally cooler indoor environment, ranging from +0.06 to -1.7 K (Table 58). A general trend was identified during which most cooling was experienced in the cold winter months, being June (-1.7 K) and July (-1.27 K), while a slight cooling effect was documented in the hotter months. In January,

typically the hottest month of the year, a negligible increase of +0.06 K was noted. The comparison revealed that the retrofitted RTGs contribute to a slightly cooler indoor environment on the top floor.

The cooler indoor environment of the retrofitted building can result from a series of factors. An analysis of the thermal gains reveals a negligible change to the indoor solar gains, but much larger changes can be ascribed to differences in internal and external conductance (Figure 99). This reveals that the RTGs generally lower the indoor thermal gain through conductance by providing added shading and adjusting the albedo factor of the roof, and improving the insulation and limiting thermal emittance by functioning as a large thermal buffer. It is important to note, the higher thermal insulation in the roof structure limits the impact of the thermal energy retained by RTGs. In section 3.2 the impact of retrofitting a poorly insulated roof is discussed.

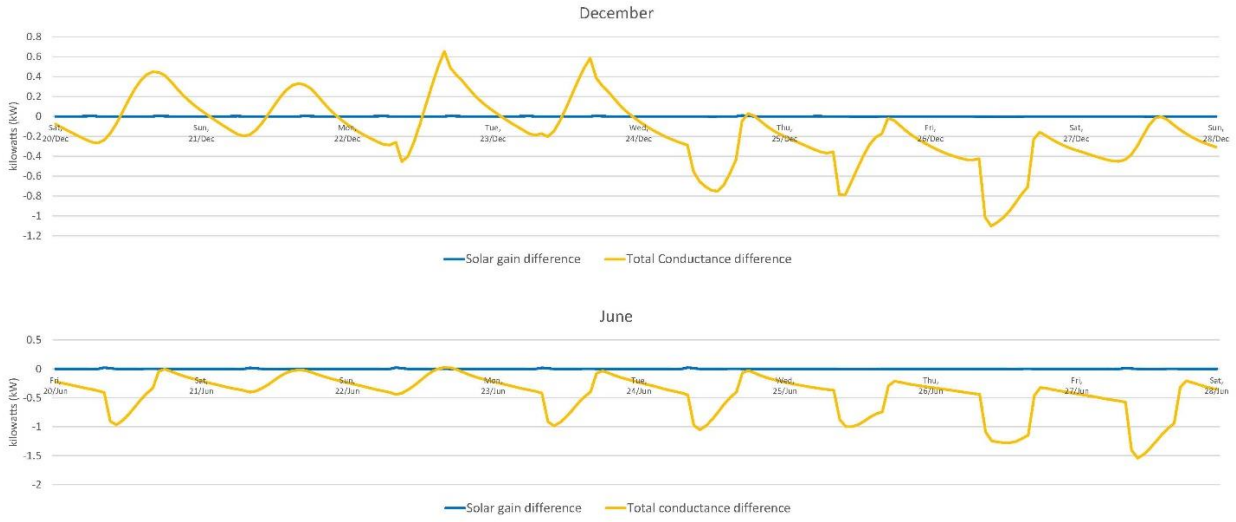

Figure 99: Difference in solar gains and conductance (A2 - A1).

Table 58: Temperature variations between the typical building (A1) and the retrofitted building (A2).

Measurement period	**Ave temp diff (K)**	**Max Temp (K)**	**Min Temp (K)**	**Diurnal swing base case vs retrofitted (K); (% increase)**
December 20-27	(-) 0.476	+ 0.69	(-) 2.06	3.01 vs 3.63 (+21%)
January 20-27	+ 0.06	+1.99	+ 0.07	3.65 vs 4.21 (+15%)
March 20-27	(-) 0.517	+0.0	(-) 1.79	3.92 vs 4.63 (+18%)
June 20-27	(-) 1.7	(-) 1.07	(-) 3.08	3.86 vs 4.26 (+10%)
July 20-27	(-) 1.27	(-) 0.62	(-) 2.15	4.23 vs 4.69 (+10%)
September 20-27	(-) 0.10	+ 0.84	(-) 0.88	3,89 vs 4.54 (+17%)

The analysis found that the added RTGs do not stabilise the indoor environment, but has a slight negative impact on the diurnal swing. The analysis revealed that the average diurnal swing increased between 10% and 21% (Table 58). The largest daily diurnal swing was on the 20th of December, when it increased by 66% compared to the A1 model (3.76 vs 2.27 K). While the retrofitted RTGs increased the average diurnal swing, smaller diurnal swings were documented at times; the most effective instance was noted on 23 January with a 15 % decrease in the diurnal swing (3.36 vs 3.87 K) compared to the A1 model.

The thermal performance analysis of an RTG retrofitted to a building with higher insulation standards revealed limited changes in absolute terms. Yet, evidence of a generally cooler indoor environment resulting from the additional RTGs has been noted, supporting arguments of negligible climate change adaptation co-benefits resulting from the retrofitting strategy.

3.2. Temperature variations of models B1 and B2

The findings from models A1 and A2 reveal that RTGs, as currently constructed and managed in Johannesburg (see chapter7), result in a slightly cooler indoor environment. While A1 and A2 models were both highly insulated (SANS 10400XA compliant), several of the buildings typically located in formalised neighbourhoods in South African cities were constructed prior the promulgation of SANS 10400XA regulations in 2011. The simulations tested whether these specific RTGs hold any benefits for buildings with poorer insulation standards (Models B1 and B2).

In terms of a visual assessment of the temperature variations of B1 and B2, the additional RTGs provided little thermal benefit. The dry-bulb temperatures simulated on the top floor of the retrofitted building (Model B2) correspond with the temperature variations of the non-retrofitted building (Model B1), and only exceeding the temperatures of B1 marginally, frequently increased the minimum indoor temperatures (Figure 100).

Table 59: Correlational analysis of the specific weeks simulated in models B1 and B2.

Period of measurement	Pearson's R	Coefficient of Correlation
December 20-27	0.99	99%
January 20-27	0.99	99%
March 20-27	0.99	99%
June 20-27	0.99	99%
July 20-27	0.99	99%
September 20-27	0.99	99%

Unfortunately, the correlational analysis of the temperature variations, between the indoor temperatures of models B1 and B2, revealed little significant change as all simulated periods showed a correlation coefficient of 0.99 (Pearson's R) (Table 59). On the whole it confirms the visual assessment's conclusion that there is little temperature variation resulting from retrofitting the structure with RTGs.

The analysis of the average indoor dry-bulb temperature conditions of Models B1 and B2 revealed that the top floor of the retrofitted building was consistently warmer than the non-retrofitted building. Resulting in the average indoor temperatures being between 0.35 to 0.61 K warmer on the top floor of the retrofitted building (Table 60). In terms of the maximum and minimum temperature variations, the retrofitted RTGs did not excessively increase the temperatures, with the maximum temperatures only increasing between 0.44 to1.20 K. Notably, the highest temperature increases occurred during the hottest months, December and January, while the lowest temperature increases were in June and July (Table 60). The deviations in terms of minimum temperatures were slightly varied ranging between -0.14 (in March) to +0.33 K (September). The indoor thermal comparison revealed a limited degree of average temperature differences resulting from the retrofitted RTGs.

Table 60: Temperature variations between the typical building (B1) and the retrofitted building (B2).

Measurement period	**Ave temp difference (K)**	**Max Temp (K)**	**Min Temp (K)**	**Diurnal swing base case vs retrofitted (K); (% increase)**
December 20-27	+ 0.53	+0.91	+ 0.18	7.04 vs 7.21 (+2%)
January 20-27	+ 0.58	+1.20	+ 0.14	6.62 vs 6.80 (+3%)
March 20-27	+ 0.49	+0.59	(-) 0.14	7.57 vs 7.83 (3%)
June 20-27	+ 0.35	+ 0.44	(-) 0.08	7.86 vs 7.94 (1%)
July 20-27	+ 0.45	+ 0.52	+ 0.26	10.28 vs 10.39 (1%)
September 20-27	+ 0.61	+ 0.68	+ 0.33	9.60 vs 9.77 (2%)

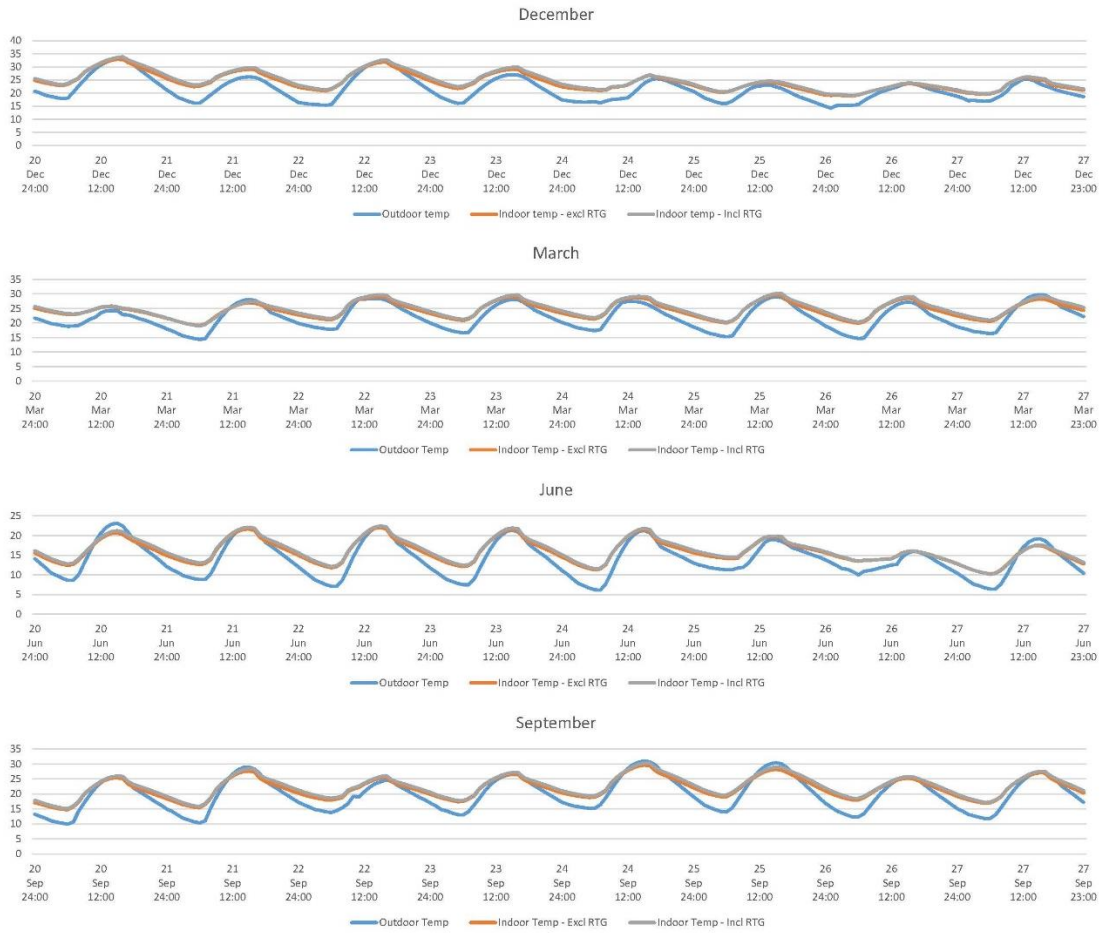

Figure 100: Temperature variations between models B1 (excl. RTGs) and B2 (incl. RTGs).

In terms of stabilising the diurnal swing, retrofitting an existing poorly insulated structure with an RTG had a minor impact on the resultant temperature variations. During all the test periods the average diurnal swing was marginally worse, effectively increased with 0.2°C (Table 60). The comparison of the daily temperature variations revealed a diurnal swing ranging from a 3% improvement on 25 June, to a 7% poorer performance on 20 February compared to model B1.

The thermal variation analysis of models B1 and B2 revealed that the added RTGs had a small but negative thermal impact on the top floor if retrofitted to an existing poorly insulated structure. In contrast to the beneficial impact of retrofitting a well-insulated building (models A1 and A2), the lower roof insulation results in the retained thermal energy in the RTG being conducted into the building interior. As a result, an increase in thermal conductance was documented in the retrofitted building (B2) (Figure 101). The findings revealed that the poorer roof insulation fails quickly during periods of overheating, effectively negating any benefits that the additional shading and changes in albedo factor of the RTGs provide. While the thermal

impact was marginal, the resultant energy consumption impact due to the retrofitting strategy is discussed in sections 3.3 and 3.4.

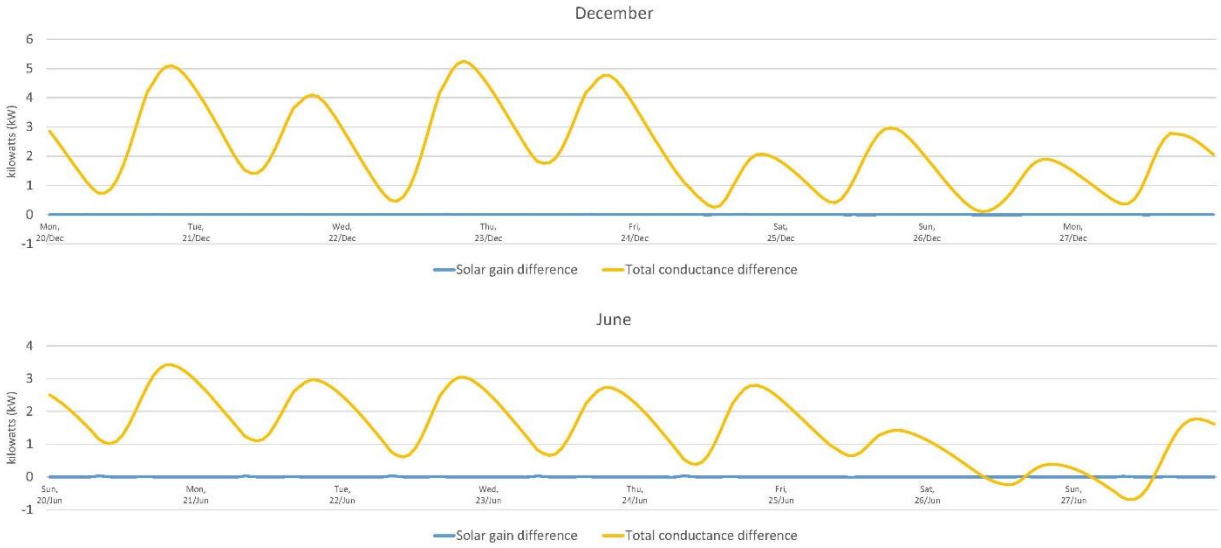

Figure 101: Differences in solar gain and thermal conductance (B2-B1).

3.3. Comparison of energy consumption between models A1 and A2

The thermal variation comparisons between the four models revealed diverging impacts resulting from the retrofitted RTGs. The highly insulated simulations (A1 & A2) reported lower indoor thermal conditions once retrofitted, while the poorly insulated simulations proved otherwise. While the intention of the study was not to develop a thermally comfortable model through passive means, the analysis aimed to quantify the energy consumption resulting from the retrofitting strategy. To understand the energy use implications of retrofitting RTGs, a series of models simulated the energy use of a basic air-conditioning system (see Table 56 for details). This was considered for both model types A1 and A2 that comply with SANS 10400XA standards.

The first analysis compared the overall building energy use. In contrast to the thermal analysis that identified a cooler indoor environment resulting from the retrofitting, the simulation revealed that the addition of the RTGs have a small but negative impact: over a full-year period the energy per square meter increased with 3.3% (105.6 vs 109.14 kWh.m^2/p.a.) (Table 61). This increase was most pronounced during the peak energy use period, when the maximum increase in energy consumption was 4.1%. This typically occurs during the December periods when extensive cooling is required (Figure 102). This increase in energy use can be attributed to the water pumps reticulating the nutrient mix in the hydroponic system (2.2% increase) as well as an increase in air-conditioning related energy use (1.1%).

Table 61: Comparison of overall building energy consumption - models A1 and A2.

Period	Model A1	Model A2	Variation	Maximum Energy Load Variation*
Full Year	105.60kWh/m^2 per year (Total: 300,972 kWh)	109.14kWh/m^2 per year (Total 311,043 kWh)	+3.3%	+4.1%
Dec	(Total: 31,019 kWh)	(Total: 32,444 kWh)	+4.6%	+4.1%
Mar	(Total: 29,510 kWh)	(Total: 30,537 kWh)	+3.5%	+3.1%
Jun	(Total: 18,967 kWh)	(Total: 19,167 kWh)	+1.0%	-2.0%
Sept	(Total: 25,358 kWh)	(Total: 26,171 kWh)	+3.2%	+3.2%
*The maximum load variation is based on the single hour with the highest energy load during the prescribed period.				

In Table 61 the analysis evaluated the changes in energy consumption during the summer and winter solstice, and equinox months. It confirmed that the highest increase in energy consumption was during the summer and autumn periods, being December and March, with increases of 4.6% and 3.5% respectively (Figure 102). The lowest energy increase occurred during the cold periods, with an increase of 1.0% in June. During this period the maximum energy load was lower, resulting in a maximum energy consumption saving of 4.5% (Figure 102). This indicates that less energy is needed for heating during the colder periods.

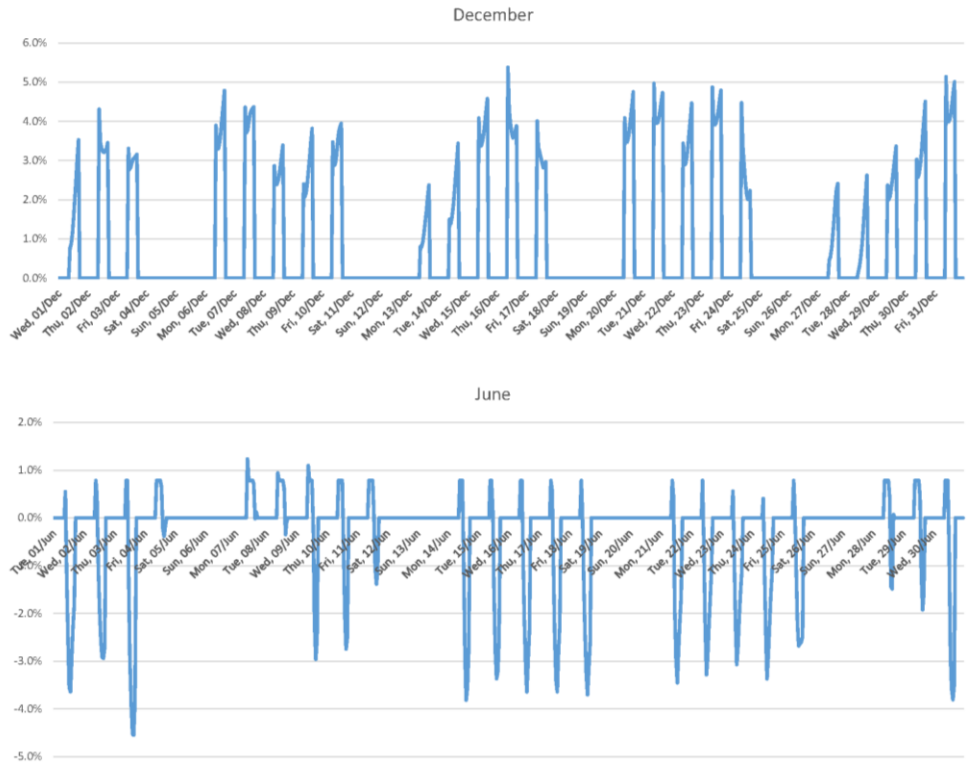

Figure 102: Comparison of energy consumption variations during June and December for models A1 and A2.

While the overall building energy consumption might be impacted to a smaller degree, further analysis considered the cooling and heating load requirements of the top floor over a full year period. The analysis specifically considered the top floor as being the most affected by the retrofitting strategy.

Table 62: Comparison of the cooling and heating loads on the top floors of models A1 and A2.

	Model A1	**Model A2**	**Variation**
Cooling Load	36,998 kWh	40,545 kWh	+9.6%
Heating Load	0.0 kWh	23 kWh	N/A
Total Load	36,998 kWh	40.568 kWh	+9.6%

The analysis revealed that adding RTGs resulted in an energy increase of 9.6%. This is primarily associated with the increased cooling needs due to the higher temperatures within the rooftop greenhouses above the spaces (Table 62). In section 3.1 the study concludes that the retrofitting of the RTGs on a highly insulated roof structure results in lower indoor temperatures, yet the addition of an air-conditioning system resulted in increased cooling loads. This can be attributed to the lower indoor temperatures maintained under air-conditioned conditions (under unconditioned circumstances the indoor temperature of the top floor is on average 5-10 K higher). The energy transfer through conductance can be defined as per Fourier's Law:

$$Q = \frac{k.(T_1 - T_2).At}{L}$$

In this case Q represents Watts (J/s), A is the total area subjected to the thermal difference (m^2), k refers to the thermal conductivity constant ($W.m^{-1}k^{-1}$), L represents the thickness of the material or entity (m), t represent the total time period of exposure (s), and $T_1 - T_2$ is the temperature gradient (K) (Ghoshdastidar 2012). This equation, therefore, shows that a higher thermal difference between two volumes through which thermal conductive transfer occurs can result in a significant increase in the amount of energy transferred.

As a result, the higher energy retained in the RTGs during the daytime, coupled with the occupation schedule of the office, leads to an increase of thermal energy being conducted into the building interior specifically at times when cooling is required. In effect the thermal insulation in the roof structure fails early during periods of overheating, transferring the added heat into the building interior, finally, translating into higher cooling loads. Figure 103 shows that this phenomenon is distinctly associated with warmer seasons. On the other hand, it is important to note that the RTG not only provides additional heat, but also shades the structure,

resulting in an increase in heating loads (Table 62; Figure 103). Notably, in absolute terms the increase in heating loads is negligible.

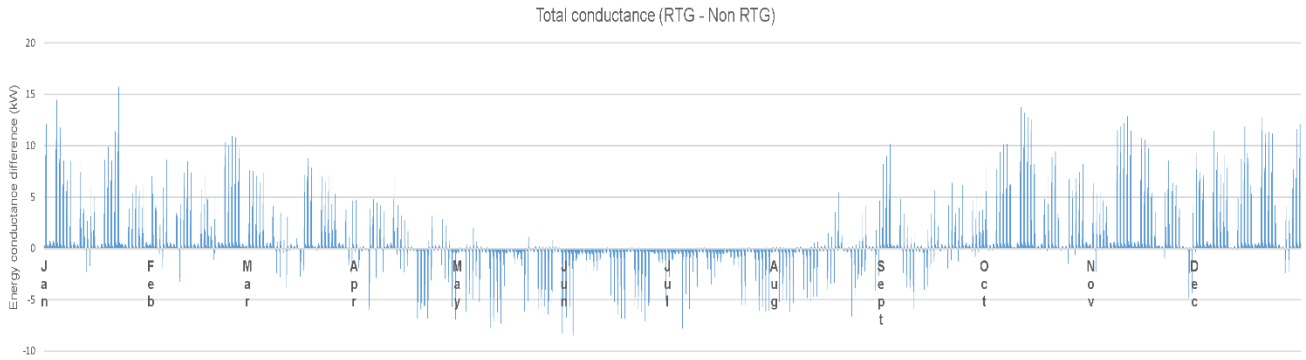

Figure 103: Total conductance difference between retrofitted and non-retrofitted simulations for models A1 and A2.

In conclusion, this simulation revealed that while the overall energy impact is limited in the models A1 and A2, the energy use impact on the floor directly below the retrofitted RTG results in a significant cooling load increase of 9.6%. This highlights the need for improved RTG designs to harness their potential co-benefits as postulated by Sanye-Mengual et al. (2018).

3.4. Comparison of energy consumption between models B1 and B2

The simulation of a poorly insulated building revealed that the addition of RTGs results in higher indoor temperatures (section 3.2). In order to further understand the impacts such higher temperatures have on the energy consumption, changes in air-condition related energy consumption were modelled (Models B1 & B2).

The analysis of the overall building energy consumption of the models B1 and B2 revealed an energy increase of 3.1% (100.09 vs 103.27 kWh/m^2/p.a.) over a full-year period. The highest energy increase was documented over the hottest periods (21 Sept - 21 March), while June experienced the lowest energy consumption impact (Table 63). Finally, in terms of air-conditioning related energy use, both the highly insulated (SANS 10400XA compliant) and the poorly insulated models were similarly affected by the RTGs.

Table 63: Comparison of overall building energy consumption - models B1 and B2.

Period	Model B1	Model B2	Variation	Maximum Energy Load Variation*
Full Year	100,09kWh/m^2 per year (Total: 285,254 kWh)	103,27kWh/m^2 per year (Total 294,319 kWh)	+3.1%	+1.9%
Dec	(Total: 29,800 kWh)	(Total: 30,770 kWh)	+3.3%	+1.5%
Mar	(Total: 25,912 kWh)	(Total: 26,682 kWh)	+2.9%	+1.0%
Jun	(Total: 21,847 kWh)	(Total: 22,433 kWh)	+2.7%	+0.0%
Sept	(Total: 22,044 kWh)	(Total: 22,789 kWh)	+3.4%	+2.0%
*The maximum load variation is based on the single hour with the highest energy load during the prescribed period.				

In terms of the energy consumption comparison (energy use difference between B1 and B2), Figure 104 reveals changes in energy use to ensure a comfortable indoor environment. During the June period, which typically requires more heating, the maximum energy consumption increase was rarely above 1%. Conversely, during the hotter September period several days require energy increases of above 2%, highlighting that RTGs function marginally better during colder periods.

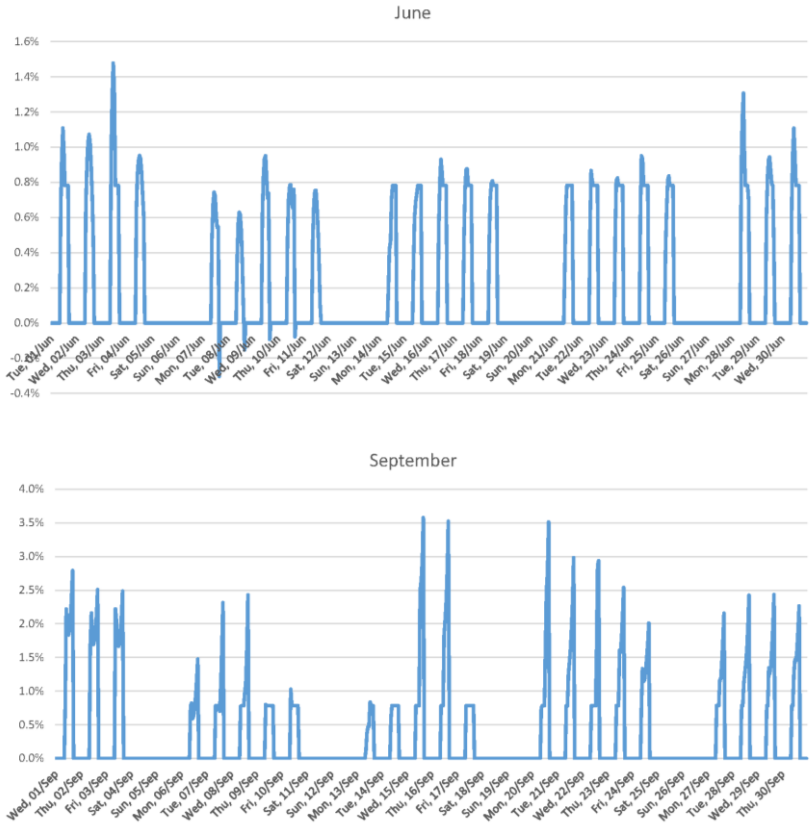

Figure 104: Comparison of energy consumption variations during June and September for models B1 and B2.

Table 64: Comparison of the cooling and heating loads on the top floors of models B1 and B2.

	Model B1	**Model B2**	**Variation**
Cooling Load	25,735 kWh	30,274 kWh	+17.6%
Heating Load	8,775 kWh	8,504 kWh	-3.1%
Total Load	34,510 kWh	38,778 kWh	+12.4%

The retrofitted RTGs led to an overall adverse impact on the sensible heating and cooling loads on the top floor, and resulted in a 12.4% overall heating and cooling load increase (Table 64). This is a proportionately larger impact than what was documented in the A1 and A2 models (Table 62). While the RTGs lowered the sensible heating load with 3.1%, the sensible cooling load increased with 17.6%. In absolute terms, this also resulted in a 27% increase in energy consumption (B2 vs B1 = 4,268; A2 vs A1 = 3,570 kWh) (Tables 62 & 64).

Consequently, the comparisons revealed that retrofitting passively controlled, non-integrated RTGs to buildings in temperate conditions with hot summers (Köppen-Geiger: Cwa) does not improve the energy consumption performance of their host buildings. While the overall energy consumption is only marginally affected, unfortunately the sensible cooling and heating loads of the top floors are significantly worse. This was evident both in proportional and absolute terms in both simulation models. This correlates with the findings by Benis et al. (2015),which state that buildings retrofitted with RTGs perform better in colder climates than under hot conditions. Unfortunately, as soon as the models are exposed to climatic conditions that require cooling, the RTGs have adverse impacts on the indoor environment. To counter this, these RTGs must be appropriately adjusted to the context and integrated with the overall building metabolism.

3.5. Analyses of models based on climate change projections

To understand the capacity of BIA to ameliorate climate change impacts, a series of simulations tested models A1, A2, B1 and B2 within projected climate change conditions. These simulations were undertaken under 2100 climate conditions as projected in A2 scenarios that replicate business-as-usual conditions within the South African context (IPCC 2000). These findings were compared to simulations of the current climatic conditions, as discussed in sections 3.1 to 3.4.

While the models did not intend to achieve thermal comfort through passive means, the documentation of the indoor dry-bulb temperatures of the various models' top floors provided insight into how the retrofitting strategies perform under higher thermal conditions. As

illustrated in Table 65, the simulations revealed that retrofitting highly insulated buildings with RTGs increase interior temperatures by up to 1.32 K. This was in contrast to the simulations under current conditions that found retrofitting these highly insulated buildings lowered the indoor thermal conditions (see section 3.1). Under the higher thermal conditions, marginally worse impacts were documented. The poorly insulated models resulted in limited temperature increases of between 0.42 to 0.72 K. The comparison revealed that the better insulated models were more affected by the addition of RTGs on the roof structure under hotter conditions.

When comparing these results with the current climate models discussed in section 3.1 and 3.2, the A2 (SANS 10400XA compliant) model shifted from providing a cooling co-benefit from the RTG's to a thermal condition that marginally increases the higher ambient temperatures and intensifies the exposure of the building-users to these higher thermal conditions. In contrast, the performance of the B2 models was very similar under both current and 2100 conditions (Table 65).

Table 65: Comparison of the thermal performance of models A1 vs A2, and B1 vs B2, under 2100 Scenario A2 conditions.

	20-27 Dec	20-27 Jan	20-27Mar	20-27 Jun	20-27 Jul	20-27 Sep
A1 ave temp (°C)	35.10	36.03	35.30	26.76	26.40	32.37
A2 ave temp(°C)	35.32	37.35	35.54	26.70	26.17	33.36
Temp Variation (K) - 2100	+ 0.22	+ 1.32	+ 0.24	(-) 0.06	(-) 0.22	+ 0.98
Temp Variation (K) – current*	(-) 0.48	+ 0.06	(-) 0.52	(-) 1.70	(-) 1.27	(-)0.1
B1 ave temp (°C)	27.40	30.10	28.19	19.62	19.70	26.24
B2 ave temp (°C)	27.82	30.80	28.68	20.10	20.14	26.97
Temp Variation (K) - 2100	+ 0.42	+ 0.69	+ 0.49	+ 0.48	+ 0.44	+ 0.72
Temp Variation (K) – current*	+ 0.53	+ 0.58	+ 0.49	+ 0.35	+ 0.45	+ 0.61
*See section 3.1 and 3.2, as well as Tables 58 and 60 for more information regarding the simulations based on current climatic conditions.						

To understand the resultant impact of such temperature differences the analysis compared the energy consumption of the four models. The analysis also compared the findings from the 2100 climate change affected simulations with the findings from the current climatic condition simulations (Sections 3.3 and 3.4). Table 66 discusses the performance of both models A1 vs A2 and B1 vs B2. First of all, while the A1 & A2 models performed better within the projected higher climate, the impact of retrofitting the roof with RTGs was worse (energy consumption

increase of 3.8% [2100] vs 3.4% [current]) (Tables 61 & 66). The simulation also substantiated that an increased adverse impact was experienced during the hot periods; in this case, in December there was a 4.6% energy consumption increase (Table 66).

While the models B1 and B2 performed much worse during the 2100 climate simulation in absolute terms, the analysis revealed that retrofitting a poorly insulated building with RTGs did not proportionally accentuate the adverse impacts as noted in models A1 and A2. The energy consumption increases for the poorly insulated models were often similar in proportion and absolute numbers under both climate conditions (Tables 62 & 66).

In terms of the sensible cooling and heating loads for the top floor, the 2100 simulation – as per the other simulations – indicated that the top floor was highly effected. The sensible cooling load increases for models A1 and A2 in the 2100 simulation were, in absolute terms, nearly double the existing conditions (3,547 vs 7,568 kWh; +9.6 vs +14%) (Tables 62 and 66)[6]. The RTG retrofitting strategy in B2 models performed better, with the proportional adverse impact lowered to only an 11.9% cooling load increase and a 5.5% heating load saving. Yet in absolute terms the sensible cooling loads of the B2 model increase significantly in the 2100 conditions (see section 3.4 for findings of existing climatic conditions). As a result, the retrofitting strategy performed only marginally better in the poorly insulated buildings than the highly insulated structures.

[6] See section 3.3 for findings of existing climatic conditions.

Table 66: Comparison of the energy consumption and heating and cooling loads of models A1 vs A2 and B1 vs B2 under 2100 scenario A2 conditions.

	Energy Use – Full building (kWh.m^2.pa)	Energy increase December (kWh)	Energy increase June (kWh)	Cooling load (top floor only) (kWh)	Heating Load (top floor only) (kWh)	Total heating and cooling
A1 (°C)	123.67	35,363	21,574	56,025	0.0	56,025
A2 (°C)	128.41	37,105	21,709	63,593	0.0	63,593
Energy Use Variation (%) - 2100	+ 4.74 (+3.8%)	+ 1,742 (+ 5.0%)	+ 135 (+ 0.1%)	7,568 (+ 14%)	0.0 (0%)	7,568 (+ 14%)
Energy Use Variation (%) – 2020*	+ 3.53 (+ 3.4%)	+ 1, 425 (+ 4.6%)	+ 200 (+1.0%)	3,547 (+ 9.6%)	23 (n/a)	3,570 (+ 9.6%)
B1 (°C)	132.01	41,706	19,056	64,501	1,592	66,093
B2 (°C)	136.19	42,957	19,641	72,182	1,505	73,687
Energy Use Variation (%) - 2100	+ 4.18 (+ 3.2%)	+ 1,251 (+ 3.0%)	+ 585 (+ 3.0%)	+ 7,681 (+11.9%)	(-) 87 (- 5.5%)	+ 7,594 (+11.5%)
Energy Use Variation (%) – 2020*	+ 3.18 (+ 3.1%)	+ 970 (+ 3.3%)	+ 586 (+ 2.7%)	+ 4,539 (+17.6%)	(-) 272 (-3.1%)	+ 4,267 (+12.4%)
* See section 3.3 and 3.4, as well as Tables 61-64 for more information regarding the simulations based on current climatic conditions.						

In terms of the retrofitted structures' overall performance, under 2100 climate change conditions, the simulation revealed an overall negative impact. While the impact in terms of energy use was marginal, there is not a clear benefit in terms of the thermal performance or energy use of both poorly and highly insulated models. Furthermore, while it might seem that retrofitted poorly insulated buildings with high infiltration rates perform better under the 2100 climate conditions, in absolute terms the highly insulated building performs significantly better (a 5.8% improvement in total, see Table 66). However, retrofitting poorly and highly insulated buildings for the added benefit of growing produce and increased functional intensity in the city, has a small, but negative, impact or cost to the building users within the projected climate change conditions. In the long term, unlike poorly insulated buildings, the adverse impact appears to increase in highly insulated structures.

4. Discussion of findings

This final research objective intended to assess the impact that a BIA farm, in this case an RTG, has on the indoor thermal environment of a building. Assessing the impact was deemed necessary as above-average global temperatures can be expected for the South African interior regions (DEA 2013). Furthermore, from the series of adverse climate change-driven impacts projected for this region, the thermal exposure can be directly addressed by the built environment and the specific retrofitting strategy. It is important to note that the study specifically considered current BIA precedents implemented in Johannesburg and Tshwane. These examples were passively controlled RTGs (ventilation through high air infiltration rates) that are not fully integrated with the built environment and function in hot and dry climatic conditions (Köppen-Geiger: Cwa).

Several studies have considered the benefits of RTGs. These studies identified a range of resource use benefits once an RTG is completely integrated with the building itself – effectively functioning as part of the building's metabolic system (Benis et al. 2017; Nadal et al. 2018; Sanye-Mengual et al. 2018). A study by Nadal et al. (2017) finds the integrated RTGs also perform better than conventional greenhouses located on ground level. However, it is vital to note that these successful cases are specifically integrated into the built environment. As identified in earlier work that Benis et al. (2015) undertook in the Mediterranean region, merely positioning a greenhouse on top of a roof has an adverse thermal impact on the interior during the hot summer season. This study supports this finding.

This simulation considered two building conditions. The first being a building that is highly insulated and has a low infiltration rate as per SANS 10400XA performance standards, while the second is considered an existing poorly insulated building that follows older building practices prior to the promulgation of SANS 10400XA's standards. In all the simulations the retrofitting strategy minimally affected the building's thermal performance and energy use; importantly though, not all the simulations revealed negative impacts resulting from the retrofitted RTGs.

The initial analysis of the highly insulated building simulation (A1 & A2) revealed a lower indoor temperature resulting from the added RTGs, notably a lower average temperature was documented in June (-1.7 K). Subsequent simulations revealed contrasting results, the simulation of a poorly insulated building revealed a slightly higher indoor temperature in September (+0.61 K). While one deduction points towards the need for improved thermal insulation between the RTGs and the building to limit any adverse impacts, subsequent simulations that tested air-condition related energy consumption proved otherwise. The simulations concluded that adverse impacts were noted due to not actively managing the

indoor environment of the RTGs. In these simulations the indoor environments' lower temperatures lead to all the simulations, including A1 and A2, resulting in higher cooling loads after being retrofitted with RTGs. While the overall energy impact might be considered low, ranging between 3.1% to 3.2% increases, the impact on the top floor was more striking. The energy use comparison revealed that the sensible cooling loads of the poorly insulated models increased significantly (+ 17.6%) when RTG structures were added to the roofs.

These findings conclude that the adverse impacts result from the building properties (in this case the insulation properties of the roof), but also from the unmanaged residual heat within the RTG's that increase the thermal conductance. As a result, one cannot assume that additional thermal energy retained in the built environment will not negatively affect adjacent interior conditions. Importantly, the residual heat provides utilisation opportunities as free heat for hot water, or alternatively storing it for later use in the RTG or in the building itself. Finally, if one can control the thermal energy and transform it into potential energy utilised within the adjacent built environment, a potential positive impact on the heat balance in the immediate urban environment can be expected.

Developing contextually appropriate design solutions is important. The analyses revealed that improvements were only documented during the coldest periods (June/July) during which additional heating would be required; therefore the results substantiate the notion that RTGs as a retrofitting strategy negatively affects the built environment in regions with dry, hot conditions (Benis et al. 2015). Sanye-Mengual et al. (2018) identify a similar trend where energy saving yields are significantly higher (38%) in cold climates than in hot climates. The study further argues that while the residual heat can be used to supplement the heating needs of the built environment in cold climates, in hot climates the added heat can be used to increase crop yields (Sanye-Mengual et al. 2018). However, the findings from a study by Thipe et al. (2017), which considered the performance of conventional passive ventilated greenhouses in arid conditions, and conversations with farmers, as discussed in Chapter 6, warn of the complexity and risks around crop management under these significantly higher thermal conditions. While the optimal temperature for plants differs, leafy greens (such as lettuce grown in many of the farms documented in the study) generally require a maximum crop canopy temperature of 24°Celsius (Peet 1999). This can be slightly higher should the temperature of the nutrient mix for the hydroponic system be managed (Graamans 2018). Yet one of the South African rooftop farmers noted that his crops were negatively affected in temperatures of above 28°C (Respondent 9, 21/04/2018). Therefore, thermal control is essential in greenhouse designs.

Notably, this study also concludes that a CCA strategy that proves beneficial under current conditions (simulations A1 & A2), can shift into negative states where the same strategy turns into a maladaptation under higher thermal conditions as simulated under A2 conditions in 2100. As noted earlier, not actively managing the residual heat retained in the greenhouse leads to increased adverse impacts under climate change affected conditions. The simulations under climate change conditions (A2 scenarios) conclude that the retrofitting strategy has a much larger negative impact, +1.32 K, on highly insulated buildings than on poorly insulated buildings. In these cases, the RTGs exacerbate the hot conditions by retaining the thermal energy and transferring it to the building interior. The lower insulated buildings are less affected, due to its increased capacity to radiate and expel thermal energy.

Care must be taken not to consider highly insulated buildings (SANS 10400XA compliant) as problematic to future climate change impacts, as the analyses revealed that the poorly insulated buildings perform much worse in terms of their energy consumption intensity compared to the former. This becomes relevant in instances where air-conditioning systems are planned or installed in buildings. On the other hand, in cases where passive climate control strategies are employed, the additional thermal insulation as an isolated strategy does not provide more thermal control benefits and the addition of RTGs further increases the indoor temperatures under higher thermal conditions.

Finally, the simulations showed that the highly insulated models (A1 and A2) are proportionally more affected by the retrofitting strategy than lower insulated models (B1 and B2). Yet in absolute terms, the lower insulated models still performed worse in the long term. Overall, these findings do not negate from the fact that the energy performance and thermal control benefits from retrofitting a structure with RTGs are limited.

5. Conclusion

Chapters 7 and 8 address the third research objective that undertook to model and assess the potential of BIA to improve the heating or cooling loads of the built environment. This involved documenting and monitoring the thermal performance of RTGs (a BIA farm type) that are currently implemented in Johannesburg and Tshwane, as well as simulating this land-use form in order to test its impact on the built environment. The overall findings reveal that passively controlled, non-integrated RTGs have generally small but negative impacts on the built environment in the Hatfield context.

Notwithstanding, the analysis emphasises the importance of identifying the appropriate technological response, testing its resultant impact, and adjusting it to the relevant context before enrolling it as a CCA strategy. It aims to prevent, as noted by Goldstein et al. (2016), claims made in the urban agriculture discourse that are non-validated assumptions. While the

use of these specific RTGs as BIA strategy can be considered a climate change maladaptation in the Hatfield context, a more nuanced holistic approach must be undertaken. This should involve a complete understanding of the range benefits and opportunities that BIA projects present, as well as considering how the technology can be adjusted to maximise the benefits. This is discussed in the next chapter that synthesizes findings from objectives A, B and C in order to understand the CCA potential of retrofitting existing buildings in the Hatfield neighbourhood with BIA farms.